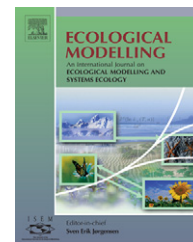


available at www.sciencedirect.comjournal homepage: www.elsevier.com/locate/ecolmodel

Estimating the biogenic enhancement factor of weathering using an inverse viability method

Werner von Bloh*, Christine Bounama, Klaus Eisenack, Brigitte Knopf, Oliver Walkenhorst¹

Potsdam Institute for Climate Impact Research (PIK), P.O. Box 601203, D-14412 Potsdam, Germany

ARTICLE INFO

Keywords:

Global carbon cycle
Weathering
Viability theory
Cambrian explosion

ABSTRACT

To determine the influence of the biosphere on weathering we use a dynamic model of the global carbon cycle. It takes into account the most important processes for the long-term evolution of the Earth. The model is solved under a slowly changing environment of increasing solar luminosity and volcanic activity and continental area. By comparing the model results for the global average temperature with data derived from $\delta^{18}\text{O}$ values from cherts it is possible to quantify the biogenic enhancement factor of weathering. For this purpose a newly developed inverse viability method is applied, which allows for calculating the range of possible biogenic enhancement factors consistent with the data. We find that in the Precambrian the weathering was 5.4 times lower than in the Phanerozoic era. This supports the hypothesis that the Cambrian explosion was caused by a positive feedback between the spread of biosphere, increased silicate weathering, and a consequent cooling of the climate.

© 2008 Elsevier B.V. All rights reserved.

1. Introduction

Weathering plays an important role in stabilising the Earth system against the increase of solar luminosity and was first described by Walker et al. (1981). In particular this stabilisation mechanism, strongly modified by biota, has gained recent interest (Schwartzman, 1999). The question of to what extent the biosphere is able to play an active role in stimulating the strength of the main carbon sink by weathering is crucial for an understanding of the dynamic properties of the Earth system and its evolution (Svirezhev et al., 2003). The evolution of the biosphere on Earth can be divided into two epochs: The Precambrian epoch before 0.542 Ga and the Phanerozoic epoch thereafter. Before the Cambrian life was mainly microscopic. During the Cambrian explosion complex life as a global phenomenon appeared and most modern life emerged. These life

forms have additionally amplified the weathering rates in the Phanerozoic.

In order to study quantitatively the influence of biogenic enhanced weathering we apply a dynamic model of the global carbon cycle for the long-term evolution of the Earth from the Archaean up to the present state. In extension to other studies on the carbon cycle, we use a general model for the thermal and degassing evolution acting as an additional driving force. For a prescribed evolution of the continental area it is possible to calculate global average surface temperatures. These values are compared with observational data based on $\delta^{18}\text{O}$ values of cherts (Robert and Chaussidon, 2006).

We attribute differences between the observational and model data to changes in the amplification of weathering processes related to the type of present biota. Especially the influence of primitive life forms on weathering before the

* Corresponding author. Tel.: +49 331 2882603; fax: +49 331 2882600.
E-mail address: bloh@pik-potsdam.de (W. von Bloh).

¹ The authors are in alphabetical order and contributed equally to this paper.
0304-3800/\$ – see front matter © 2008 Elsevier B.V. All rights reserved.
doi:10.1016/j.ecolmodel.2008.03.005

Cambrian era is not well understood yet and therefore difficult to parameterise. We want to estimate the extent of this biotic enhancement of weathering by modifying the model by an additional factor, which is assumed to depend only on time. This factor is calculated by applying an inverse viability method taking the modified model and the observational data for granted. Viability theory is in general well suited to investigate differential equations under constraints on their solutions. In our case, we use this approach to determine all evolutionary paths of the weathering factor that approximate the data in a specified sense. This method, based on work of Aubin (Aubin, 1991; Aubin and Saint-Pierre, 2007) and Bonneuil (Bonneuil, 1994; Bonneuil and Müllers, 1997), is innovative in its own. Although much more general, it is shown to be adequate for the analysis in this paper where a structurally uncertain relationship has to be estimated. Similar approaches are increasingly used in the field of ecological modelling (e.g. Bonneuil and Müllers, 1997) and climate change research (Petschel-Held et al., 1999).

The paper is organised as follows: in Section 2 we describe the model of the global carbon cycle for the long-term evolution, in Section 3 the data used are summarised. The inverse viability method is presented in Section 4 and in Section 5 we discuss the model results.

2. Model description

In our approach (von Bloh et al., 2003a) we consider the balance of continental spreading and volcanic emissions F_s as the main source and weathering F_{wr} as the dominant sink of carbon in the atmosphere, C_{atm} :

$$\dot{C}_{atm} = F_s - F_{wr}. \quad (1)$$

This is the key equation describing the ecosphere. The other variables of the ecosphere (surface temperature, biological productivity) can be derived from C_{atm} . In order to solve this dynamic equation it is necessary to describe the parameterisation of F_{wr} and F_s .

2.1. Parameterisation of weathering

The overall process of weathering contains first the reaction of silicate minerals with carbon dioxide, second the transport of weathering products, and third the deposition of carbonate minerals in sediments. The availability of cations plays the main role in these processes. This is the limiting factor in the carbonate sediments forming reaction (third process) between cations (Ca^{2+} and Mg^{2+}) and carbonate anions (CO_3^{2-}). Therefore, for the mathematical formulation we have only to take into consideration the amount of released cations and their runoff (first and second process). Following Walker et al. (1981), the weathering rate $F_{wr,A}$ is the product of cations concentration in water (in mass per unit volume) and runoff (in volume per unit area per unit time). Therefore, the weathering rate is the mass of cations formed per unit area and unit time. Combining the direct temperature effect on the weathering reaction, the weak temperature effect on river runoff, and the dependence of weathering on soil CO_2 con-

centration (Walker et al., 1981; Caldeira and Kasting, 1992), the silicate-rock weathering rate, as a global average value, can be formulated in the following way:

$$F_{wr} = \frac{A_c}{A_{c,0}} = \frac{A_c}{A_{c,0}} \left(\frac{a_{H^+}}{a_{H^+,0}} \right)^{0.5} \exp \left(\frac{T_s - T_0}{13.7K} \right). \quad (2)$$

The quantities $F_{wr,0}$, $A_{c,0}$, $a_{H^+,0}$, and T_0 are the present values for the weathering rate, the continental area, the H^+ activity, and the surface temperature, respectively. a_{H^+} is the activity of H^+ in fresh soil-water and is itself a function of the surface temperature T_s and the CO_2 concentration in the soil C_{soil} , where the equilibrium constants for the chemical activities of the carbon and sulphur systems have been taken from Stumm and Morgan (1981). C_{soil} can be parameterised as a function of the terrestrial biological productivity Π , the atmospheric CO_2 concentration C_{atm} , and the corresponding present values ($C_{soil,0}$, Π_0 , $C_{atm,0}$):

$$\frac{C_{soil}}{C_{soil,0}} = \frac{\Pi}{\Pi_0} \left(1 - \frac{C_{atm,0}}{C_{soil,0}} \right) + \frac{C_{atm}}{C_{soil,0}}. \quad (3)$$

One role of the biosphere in the context of our model is to increase the soil CO_2 partial pressure C_{soil} in relation to the atmospheric one. This effect is supposed to be mainly proportional to Π . This is a rather weak functional dependence of the weathering rate on biological productivity. A 10-fold increase in soil pCO_2 relative to atmosphere gives only a 1.56-fold amplification of weathering rate due to the present biota. This is a significant underestimate, indicating much of the observed biotic amplification of weathering is due to processes other than increased soil pCO_2 . According to Schwartzman (1999) the total amplification due to land life is at least a factor of 10 and may exceed 100. The weathering rate in the past might be by a factor α lower than the present weathering rates with a modern biosphere. Therefore, we introduce in Eq. (1) an additional time-dependent pre-factor $\alpha(t)$, with $\alpha(t) \in [0, 1]$:

$$\dot{C}_{atm} = F_s - \alpha(t)F_{wr}. \quad (4)$$

The factor captures all further biotic processes influencing the weathering rate that are not explicitly parameterised in the model. Since there is no valid ad hoc structural relationship between α and the other (or further) model variables, it is introduced as time-dependent. The viability method we present in Section 4 will be used to compute the set of all evolutions $\alpha(t)$ that are in accordance with empirical data. This set indirectly includes all possible parameterisations. If the weathering effect of different types of biota were negligible, the method would result in constant values for α .

2.2. Parameterisation of spreading and volcanic emissions

The sources of CO_2 into the atmosphere/ocean system are seafloor spreading at the mid-ocean ridges and back-arc or andesitic volcanism. Both processes are dependent on the spreading rate S . General models of the volatile exchange between mantle and surface reservoirs (Mc Govern and Schubert, 1989; Franck and Bounama, 1995, 1997; Franck et

al., 2000) assume that the mantle degassing as the source of CO₂ for the atmosphere/ocean system is proportional to the so-called degassing volume beneath mid-ocean ridges. This degassing volume depends linearly on the areal spreading rate S . Therefore we get for the flux F_s into the atmosphere the following relation:

$$F_s = F_{s,0} \times \frac{S}{S_0}, \quad (5)$$

where $F_{s,0}$ and S_0 denote the present volcanic flux and present areal spreading rate. The present value for $F_{s,0}$ can be estimated to 0.029–0.068 ppm/year (Berner et al., 1983; Walker and Kasting, 1992). Under the assumption that the present state of the Earth is in an equilibrium, this value is equivalent to the present rate of weathering $F_{wr,0}$. For the determination of the spreading rate a model of Franck and Bounama (1995, 1997) is used, which couples the thermal and degassing history of the Earth. Assuming conservation of energy we can write the following equation for the average mantle temperature, T_m :

$$\frac{4}{3}\pi\rho c(R_m^3 - R_c^3)\dot{T}_m = -4\pi R_m^2 q_m + \frac{4}{3}\pi Q(t)(R_m^3 - R_c^3), \quad (6)$$

where ρ is the density, c is the specific heat at constant pressure, q_m is the heat flow from the mantle, Q is the energy production rate by decay of radiogenic heat sources in the mantle, and R_m and R_c are the outer and inner radii of the mantle, respectively.

The mantle heat flow is parameterised in terms of the Rayleigh number, Ra :

$$q_m = \frac{k(T_m - 273 \text{ K})}{(R_m - R_c)} \left(\frac{Ra}{Ra_{crit}} \right)^\beta, \quad (7)$$

with

$$Ra = \frac{g\theta(T_m - 273 \text{ K})(R_m - R_c)^3}{\kappa\nu}, \quad (8)$$

where k is the thermal conductivity, Ra_{crit} is the critical value of Ra for the onset of convection, β is an empirical constant, g is the acceleration of gravity, θ is the coefficient of thermal expansion, κ is the thermal diffusivity, and ν is the water-dependent kinematic viscosity. This viscosity can be calculated with the help of a water fugacity-dependent mantle creep rate. For details of this parameterisation see Franck and Bounama (1995). The areal spreading rate is a function of the average mantle temperature, the mantle heat flow, and the continental growth model over the time-dependent area of ocean basins (Turcotte and Schubert, 1982):

$$S = \frac{q_m^2 \pi \kappa A_0(t)}{4k^2(T_m - 273 \text{ K})^2}. \quad (9)$$

The normalised spreading rate calculated from the evolution of the mantle temperature (internal driving force) and the evolution of the normalised luminosity $L(t)/L_0$ (external driving force) is shown in Fig. 1.

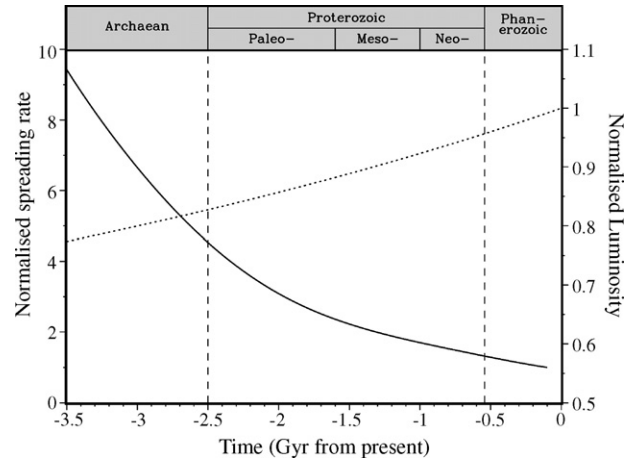


Fig. 1 – Evolution of the normalised areal spreading rate (solid line) and the luminosity (dotted line) as the driving forces of the Earth system, respectively.

2.3. Climate model

In order to calculate the atmospheric CO₂ concentration C_{atm} , we need a climate model which links the temperature to the given partial pressure of atmospheric CO₂ and the solar luminosity L . Here we apply the grey atmosphere model by Lenton (2000) (see also Chamberlain, 1980). The surface temperature T_s is determined using the energy balance between the incoming and outgoing radiation:

$$\sigma T_s^4 = \frac{(1-a)L}{4} \left(1 + \frac{3}{4}\tau \right), \quad (10)$$

where σ is the Stefan Boltzmann constant ($5.67 \times 10^{-8} \text{ W m}^{-2} \text{ K}^{-4}$), a is the average planetary albedo, and τ is the vertical opacity of the greenhouse atmosphere. The equation can be solved for atmospheric carbon by the following considerations. The opacity of the two greenhouse gases, CO₂ and H₂O, is assumed to be independent from each other:

$$\tau = \tau(p_{CO_2}) + \tau(p_{H_2O}). \quad (11)$$

The opacity of CO₂ is assumed to be a function of its mixing ratio. It is derived from the results of varying CO₂ in a radiative–convective climate model. The partial pressure of H₂O, p_{H_2O} , can be expressed as a function of temperature T_s and relative humidity H , using the Clausius–Clapeyron equation. Here we use a wet greenhouse model with $H=1$ (full saturation). The albedo, a , is a function of the surface temperature (Caldeira and Kasting, 1992) derived from least-square fits to the results of a radiative–convective climate model with $0^\circ\text{C} \leq T_s \leq 100^\circ\text{C}$:

$$a = 1.453614 - 0.0065979T_s + 8.567 \times 10^{-6}T_s^2. \quad (12)$$

The opacities $\tau(p_{\text{CO}_2})$ and $\tau(p_{\text{H}_2\text{O}})$ are calculated in the following way:

$$\tau(p_{\text{CO}_2}) = 1.73(C_{\text{atm}})^{0.263}, \quad \tau(p_{\text{H}_2\text{O}}) = 0.0126(p_{\text{H}_2\text{O}})^{0.503}. \quad (13)$$

The solar luminosity evolves according to Caldeira and Kasting (1992):

$$L(t) = L_0 \left(\frac{1 - 0.38(t - 4.55 \text{ Gyr})}{4.55 \text{ Gyr}} \right)^{-1}, \quad (14)$$

where L_0 denotes the present day value of the solar constant (1368 W m^{-2}).

2.4. Biological productivity

The biological productivity Π is itself a function of various parameters such as water supply, photosynthetic active radiation (PHAR), nutrients (e.g., N and C), C_{atm} , and T_s . In the framework of this model Π is considered to be a function of the temperature and CO_2 partial pressure in the atmosphere only and is parameterised following Svirezhev and von Bloh (1997). According to Liebig's principle Π can be set to a multiplicative form:

$$\Pi \equiv \Pi(T_s, C_{\text{atm}}) = \Pi_{\text{max}} \Pi_T(T_s) \Pi_C(C_{\text{atm}}), \quad (15)$$

$$0 \leq \Pi_T(T_s), \Pi_C(C_{\text{atm}}) \leq 1.$$

The maximum productivity Π_{max} is estimated to be twice the present value (Volk, 1987), i.e. $\Pi_{\text{max}} = 2\Pi_0$. Following Volk (1987), Michaelis–Menten hyperbolas are suitable for describing the functional behaviour of Π_C :

$$\Pi_C(C_{\text{atm}}) = \begin{cases} \frac{C_{\text{atm}} - C_{\text{min}}}{C_{1/2} + (C_{\text{atm}} - C_{\text{min}})} & \text{for } C_{\text{atm}} > C_{\text{min}} \\ 0 & \text{else} \end{cases}, \quad (16)$$

where $C_{1/2} + C_{\text{min}}$ is the value at which $\Pi_C = 1/2$, $C_{\text{min}} = 10 \text{ ppm}$. Eq. (16) tends to $\Pi_C = 1$ for $C_{\text{atm}} \rightarrow \infty$.

The temperature dependence Π_T is described by a parabolic function used by Caldeira and Kasting (1992) having a maximum at $T_s = 25^\circ\text{C}$:

$$\Pi_T(T_s) = \begin{cases} 1 - \left(\frac{T_s - 25^\circ\text{C}}{25^\circ\text{C}} \right)^2 & \text{for } 0^\circ\text{C} < T_s < 50^\circ\text{C} \\ 0 & \text{else} \end{cases} \quad (17)$$

The resulting function $\Pi(T_s, C_{\text{atm}})$ is an adequate description of the so-called net primary productivity (NPP) for the present biosphere.

3. Geological data

Weathering depends strongly on the continental area A_c . The formation of continents is not well understood because of the diverse and heterogeneous nature of the continental crust. In modern studies (see, e.g., Taylor and McLennan, 1995), there is a growing appreciation of the observation that the continental crust grows episodically. In the present paper we use a

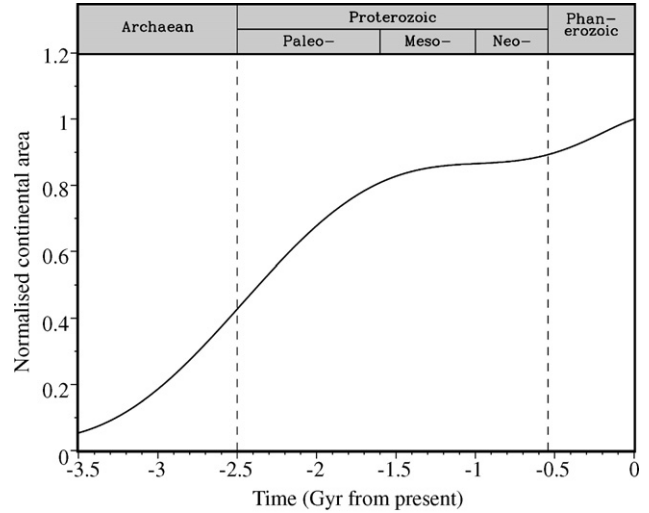


Fig. 2 – Continental growth model according to Collerson and Kamber (1999).

continental growth model that is based on geological investigations (Collerson and Kamber, 1999) inferred from Th–U–Nb systematics of the depleted mantle. The model approximates episodes of continental growth with the help of an interpolation polynomial. The resulting evolution of the continental area is shown in Fig. 2.

Data for the global average temperature have been derived from $\delta^{18}\text{O}$ values of cherts (Robert and Chaussidon, 2006). These values are used as a proxy for the ocean temperatures. The oxygen isotopic fractionation between chert and water:

$$\Delta^{18}\text{O} = \delta^{18}\text{O}_{\text{chert}} - \delta^{18}\text{O}_{\text{water}}, \quad (18)$$

depends on water temperature T_w according to the equation:

$$1000 \ln(\Delta^{18}\text{O}) = (3.09 \times 10^6 T_w^{-2}) - 3.29. \quad (19)$$

Considering that ice caps were absent, i.e., $\delta^{18}\text{O}_{\text{water}} \approx -1\text{‰}$ then temperatures can be calculated directly from $\delta^{18}\text{O}_{\text{water}}$.

Robert and Chaussidon (2006) remark that it is only necessary to consider the highest $\delta^{18}\text{O}_{\text{chert}}$ values to obtain reliable ocean temperature proxies. In order to avoid artefacts due to small sample sizes we selected the maximum value of $\delta^{18}\text{O}_{\text{chert}}$ for each interval $t \pm 0.1 \text{ Ga}$, which is covered by the samples, provided that more than one data point lies in the interval. Using this procedure we obtain 11 temperature data points between 3.5 Ga and today which are shown with their original error bars in Fig. 3.

4. The inverse viability method

Since the weathering rate F_{wr} indirectly depends on atmospheric carbon C_{atm} and $L(t)$ (via Eqs. (2), (10) and (13)), and since also F_s only depends on time (via Eqs. (5), (9) and (6)), the basic differential equation (Eq. (4)) can be rewritten as

$$\dot{C}_{\text{atm}} = F_s(t) - \alpha(t)F_{\text{wr}}(C_{\text{atm}}, t). \quad (20)$$

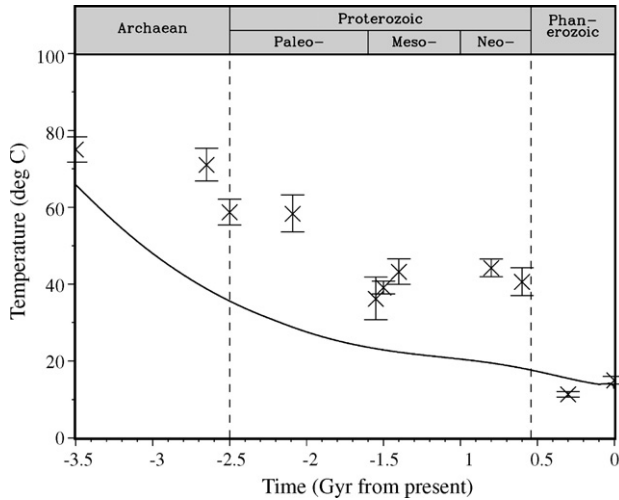


Fig. 3 – Evolution of global average temperature T_s for fixed $\alpha \equiv 1$ (solid line). The markers denote temperature estimates derived from $\delta^{18}\text{O}$ values of cherts. The vertical error bars are related to the uncertainties in the $\delta^{18}\text{O}$ measurements.

We want to determine $\alpha(t)$ using the model and the geological data for C_{atm} .

More generally, this can be formulated as a problem of the following type. We have a given ODE:

$$\dot{\mathbf{x}} = \mathbf{f}(\mathbf{x}, t, \mathbf{p}), \quad (21)$$

with a state vector $\mathbf{x} \in R^n$, a (time-dependent) parameter vector $\mathbf{p} \in P \subseteq R^m$, and a vector-valued, continuous function \mathbf{f} . In the present paper, $\mathbf{x} \equiv C_{\text{atm}}$, $\mathbf{p} \equiv \alpha$. From the empirical data, a time series $\{\mathbf{x}_t\}$ with time steps t is prescribed, in our case $\{C_{\text{atm},t}\}$. Note that by selecting an initial state \mathbf{x}_0 and an evolution of the parameter vector $\mathbf{p}(t)$, a solution of the ODE in Eq. (21) is defined (supposed that \mathbf{f} is sufficiently regular). The problem is to find the set of all evolutions $\mathbf{p}(t)$ such that the resulting solution approximates the empirical time series $\{\mathbf{x}_t\}$ in the following sense: (i) for every time τ between time steps t_i, t_{i+1} of the time series, the velocity $\mathbf{f}(\mathbf{x}(\tau), \tau, \mathbf{p}(\tau))$ is within a prescribed interval V_τ ; and (ii) for every step t of the time series, the solution $\mathbf{x}(t)$ is within a prescribed set D_t around \mathbf{x}_t (e.g. the error bars indicated in Fig. 3). The second constraint guarantees that an evolution of \mathbf{p} is only admitted if it reproduces the absolute values of the empirical data up to error bounds. The first constraint is essential to omit evolutions where \mathbf{p} and consequently \mathbf{x} are strongly fluctuating. The intervals V_τ are determined from estimates of the derivatives $\dot{\mathbf{x}}(\tau)$ based on the empirical time series.

This approach is an inverse method since it starts from an incompletely parameterised model and empirical data, and determines the quantitatively unknown parameters from that. We call it a viability method since it fits into the general framework of viability theory (Aubin, 1991). In the following paragraph we outline its most basic concepts and relate them to the present problem, making it possible to exploit results from viability theory.

For a given ODE as Eq. (21), an initial state $\mathbf{x}(t_0)$ and an evolution $\mathbf{p}(\tau)$, a resulting solution $\mathbf{x}(\tau)$ is called *viable* in the family

of sets $\{K_\tau\}$, $K_\tau \subseteq R^n$ on a time interval $J = [t_0, t_1]$ with target $D \subseteq R^n$ if (i) $\mathbf{x}(\tau)$ remains in the constrained set K_τ for all $\tau \in J$, and (ii) reaches the target $\mathbf{x}(t_1) \in D$ at the end of the time interval (cf. Aubin, 2001; Eisenack, 2006). The *viability kernel* is the set of all initial conditions $\mathbf{x}(t_0)$ such that there exists a trajectory $\mathbf{p}(\tau)$ with a viable solution. However, our ultimate target is to determine the admissible trajectories $\mathbf{p}(\tau)$ explicitly. Fortunately, it can be shown that if the problem is technically extended as follows, the viability kernel contains all trajectories of parameters \mathbf{p} that lead to viable solutions (Aubin, 1991). For that it is needed to join the state and parameter space, i.e. to consider joint evolutions $(\mathbf{x}(\tau), \mathbf{p}(\tau))$ and to modify the constrained sets K_τ such that they also include a bound on the velocity $\dot{\mathbf{p}}$. To compute the viability kernel, various sophisticated methods exist (e.g. Saint-Pierre, 1994; Cardaliaguet et al., 1999; Bonneuil, 2006). Since the problem in the present paper has a simple state space and since the model is linear in the unknown parameter, the computation is simpler.

In our case, the viability problem is solved independently for every pair of subsequent time steps (t_i, t_{i+1}) of the empirical time series, defining the time interval $J = [t_i, t_{i+1}]$. We consider the joint state and velocity space, i.e. evolutions of $(C_{\text{atm}}, \dot{C}_{\text{atm}})$. The family of constrained sets K_τ is given by the admissible velocities V_τ (while there are no constraints on the component C_{atm}) according to condition (i) above. The target $D = D_t$ is given by condition (ii) and only includes a constraint for C_{atm} and not for \dot{C}_{atm} . The derivatives $\dot{C}_{\text{atm}}(\tau)$ are approximated with standard numerical analysis methods from $\{C_{\text{atm},t}\}$, which in turn is determined via Eqs. (10) and (13) from the empirical time series $\{T_{s,t}\}$. Between time steps, $T_s(\tau)$ is linearly interpolated. The admissible velocities V_τ are set to be intervals $\dot{C}_{\text{atm}}(\tau) \pm 0.2\dot{C}_{\text{atm}}(\tau)$. Based on that the set of all $\alpha(\tau)$ that fulfill the requirements can be separately determined for each given $\tau \in J$. The result is displayed as a “corridor” (see Fig. 4). We also applied this method successfully to other models, e.g. the chaotic Lorenz system, with simulated data in this case.

5. Results and discussion

The evolution of carbon dioxide in the atmosphere $C_{\text{atm}}(t)$ has been calculated for a fixed factor of $\alpha(t) \equiv 1$ neglecting an additional influence of the biosphere on weathering. The corresponding evolution of the global average surface temperature is shown in Fig. 3. The values for the temperatures derived from $\delta^{18}\text{O}$ values of cherts are plotted. The modelled temperatures are too low compared to the observational data in particular for the Archaean and Proterozoic era. This is caused by overestimated weathering rates in the model and can be lowered by choosing a time-dependent factor $\alpha(t) < 1$ in Eq. (4). The inverse viability method can be used to determine all paths for $\alpha(t)$ that get model temperatures consistent with the geological data. The resulting factor α is plotted in Fig. 4. The Phanerozoic epoch ($0.541 \text{ Ga} < t < 0$) is characterised by a value $\alpha > 1$ while in the Proterozoic and Archaean epoch ($t < 0.541 \text{ Ga}$) the value is significantly lower than one. The average Precambrian value for α is $\bar{\alpha} = 0.18$, i.e. the weathering rate was by a factor of 5.4 lower compared to the Phanerozoic where α is assumed to be one.

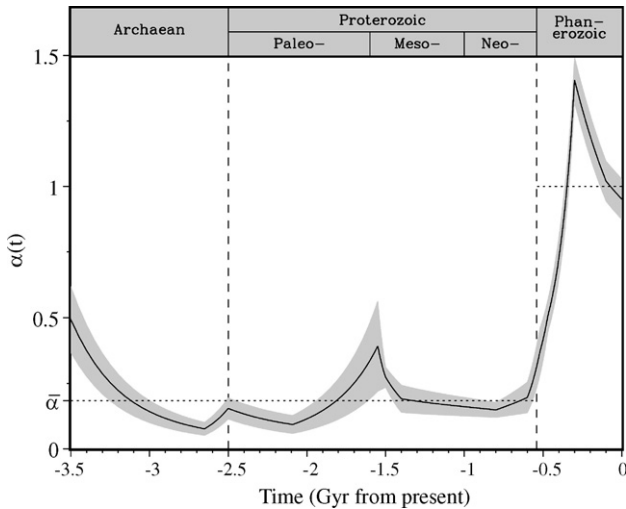


Fig. 4 – Time-dependent factor $\alpha(t)$ describing the amplification of weathering by biota derived from the inverse viability method. The grey band corresponds to the corridor of all admissible values for α that are consistent with the observed temperature data. The horizontal line denotes the average value $\bar{\alpha}$ of the Archaean and Proterozoic epoch and the Phanerozoic epoch, respectively.

In the Cambrian era we find a sharp increase of α . This finding is in line with results from von Bloh et al. (2003b). They proposed that the Cambrian explosion, i.e. the first occurrence of complex life as a global phenomenon, was so rapid because of a positive feedback between the spread of biosphere, increased silicate weathering, and a consequent cooling of the climate. If the global average temperature is just below the upper temperature tolerance limit for complex life, T_{\max} , the biosphere starts to spread increasing the weathering rate by a specific factor. Franck et al. (2006) found that for $T_{\max} = 34^\circ\text{C}$ the amplification factor can be estimated to $5.4 \approx 1/\bar{\alpha}$. Therefore, our finding supports the idea that a nonlinear feedback of the geosphere–biosphere system has caused the Cambrian explosion.

We can show that the inverse viability approach is useful for problems where a part of a model (a parameter or, in an alternative formulation, a coupled sub-model) is not completely known, but where data are available. Most importantly, this method computes all parameterisations that are consistent with the given data, and not just one. The newly introduced inverse viability method can also be applied to similar problems where a parameterisation is unknown, e.g. the parameterisation of phosphorus recycling which can contribute to lake eutrophication (e.g. Carpenter, 2003), or where the coupling between two phenomena is not fully understood, e.g. between the Indian monsoon and El Niño–Southern Oscillation (ENSO) (Webster and Yang, 1992).

Acknowledgments

Part of this work was funded by the German Research Association (DFG) (grant number PR1175/1-1).

REFERENCES

- Aubin, J.-P., 1991. *Viability Theory*. Birkhäuser, Basel.
- Aubin, J.-P., 2001. Viability kernels and capture basins of sets under differential inclusions. *SIAM Journal on Control and Optimization* 40 (3), 853–881.
- Aubin, J.-P., Saint-Pierre, P., 2007. An introduction to viability theory and management of renewable resources. In: Kropp, J.P., Scheffran J. (Eds.), *Advanced Methods for Decision Making and Risk Management in Sustainability Science*. Nova Science Publishers, New York, pp. 43–80.
- Berner, R.A., Lasaga, A.C., Garrels, R.M., 1983. The carbonate–silicate geochemical cycle and its effects on atmospheric carbon dioxide over the past 100 million years. *Am. J. Sci.* 283, 641–683.
- Bonneuil, N., 1994. Malthus, Boserup and population viability. *Mathematical Population Studies* 5 (1), 107–119.
- Bonneuil, N., 2006. Computing the viability kernel in large state dimension. *Journal of Mathematical Analysis and Applications* 323, 1444–1454.
- Bonneuil, N., Müllers, K., 1997. Viable populations in a prey–predator system. *Journal of Mathematical Biology* 35, 261–293.
- Caldeira, K., Kasting, J.F., 1992. The life span of the biosphere revisited. *Nature* 360, 721–723.
- Cardaliaguet, P., Quincampoix, M., Saint-Pierre, P., 1999. Numerical methods for differential games. In: Bardi, M., Raghavan, T.E.S., Parthasaeathy, T. (Eds.), *Stochastic and Differential Games: Theory and Numerical Methods*. Annals of the International Society of Dynamic Games, Birkhäuser, pp. 441–461.
- Carpenter, S.R., 2003. *Regime Shifts in Lake Ecosystems: Pattern and Variation*. Excellence in Ecology, vol. 15. Ecology Institute, Oldendorf, Germany.
- Chamberlain, J.-W., 1980. Changes in the planetary heat balance with chemical changes in air. *Planet. Space Sci.* 28, 1011–1018.
- Collerson, K.D., Kamber, B.S., 1999. Evolution of the continents and the atmosphere inferred from Th–U–Nb systematics of the depleted mantle. *Science* 283, 1519–1522.
- Eisenack, K., 2006. *Model ensembles for natural resource management: extensions of qualitative differential equations using graph theory and viability theory*. PhD thesis. Free University Berlin, Darwin, <http://www.diss.fu-berlin.de/2006/326>.
- Franck, S., Bounama, C., 1995. Effects of water-dependent creep rate on the volatile exchange between mantle and surface reservoirs. *Phys. Earth Planet. Inter.* 92, 57–65.
- Franck, S., Bounama, C., 1997. Continental growth and volatile exchange during Earth’s evolution. *Phys. Earth Planet. Inter.* 100, 189–196.
- Franck, S., Block, A., von Bloh, W., Bounama, C., Schellnhuber, H.J., Svirezhev, Y., 2000. Reduction of biosphere life span as a consequence of geodynamics. *Tellus* 52 (1), 94–107.
- Franck, S., Bounama, C., von Bloh, W., 2006. Causes and timing of future biosphere extinctions. *Biogeosciences* 3, 85–92.
- Lenton, T.M., 2000. Land and ocean carbon cycle feedback effects on global warming in a simple Earth system model. *Tellus* 52B, 1159–1188.
- Mc Govern, P.J., Schubert, G., 1989. Thermal evolution of the Earth: effects of volatile exchange between atmosphere and interior. *Earth Planet. Sci. Lett.* 96, 27–37.
- Petschel-Held, G., Schellnhuber, H.-J., Bruckner, T., Tóth, F., 1999. The tolerable windows approach: theoretical and methodological foundations. *Climatic Change* 41, 303–331.
- Robert, F., Chaussidon, M., 2006. A paleotemperature curve for the Precambrian oceans based on silicon isotopes in cherts. *Nature* 443, 969–972.

- Saint-Pierre, P., 1994. Approximation of the viability kernel. *Applied Mathematics and Optimization* 24, 187–209.
- Schwartzman, D.W., 1999. *Life, Temperature and the Earth: the Self-organizing Biosphere*. Columbia University Press, New York.
- Stumm, W., Morgan, J.J., 1981. *Aquatic Chemistry*. Wiley, New York.
- Svirezhev, Y.M., von Bloh, W., 1997. Climate, vegetation, and global carbon cycle: the simplest zero-dimensional model. *Ecol. Model.* 101, 79–95.
- Svirezhev, Y.M., Block, A., von Bloh, W., 2003. “Active planetary cover” concept and long-term evolution of planetary climate. In: Krumbein, W.E., Paterson, D.M., Zavarzin, G.A. (Eds.), *Fossil and Recent Biofilms, A Natural History of Life on Earth*. Kluwer Academic Publishers, Dordrecht/Boston/London, pp. 415–427.
- Taylor, S.R., McLennan, S.M., 1995. The geological evolution of the continental crust. *Rev. Geophys.* 33, 265–641.
- Turcotte, D.C., Schubert, G., 1982. *Geodynamics*. John Wiley, New York.
- Volk, T., 1987. Feedbacks between weathering and atmospheric CO₂ over the last 100 million years. *Am. J. Sci.* 287, 763–779.
- von Bloh, W., Franck, S., Bounama, C., Schellnhuber, H.-J., 2003a. Biogenic enhancement of weathering and the stability of the ecosphere. *Geomicrobiol. J.* 20, 501–511.
- von Bloh, W., Bounama, C., Franck, S., 2003b. Cambrian explosion triggered by geosphere–biosphere feedbacks. *Geophys. Res. Lett.* 30, 1963–1967.
- Walker, J.C.G., Kasting, J.F., 1992. Effects of fuel and forest conservation on future levels of atmospheric carbon dioxide. *Paleogeography, Paleoclimatology, Paleocology (Global and Planetary Change Section)* 97, 151–189.
- Walker, J.C.G., Hays, P.B., Kasting, J.F., 1981. A negative feedback mechanism for the long-term stabilization of Earth’s surface temperature. *J. Geophys. Res.* 86, 9776–9782.
- Webster, P.-J., Yang, S., 1992. Monsoon and ENSO: selectively interactive systems. *Quarterly Journal of the Royal Meteorological Society* 118, 877–926.